



Estimation of ground state and excited state dipole moments of a novel Schiff base derivative containing 1, 2, 4-triazole nucleus by solvatochromic method



Roshmy Alphonse, Anitha Varghese*, Louis George, Aatika Nizam

Department of Chemistry, Christ University, Hosur Road, Bangalore 560029, India

ARTICLE INFO

Article history:

Received 31 May 2015

Received in revised form 7 November 2015

Accepted 14 December 2015

Available online xxx

Keywords:

Solvatochromic effect

TD-DFT calculation

Solvent polarity correlation method

Dipole moment

ABSTRACT

A novel schiff base derivative containing 1, 2, 4-triazole moiety (NBTMPA) has been synthesized from 4-[1, 2, 4] triazol-1-ylmethyl-phenylamine and 4-nitrobenzaldehyde in the presence of glacial acetic acid in an ethanolic medium. The absorbance and fluorescence spectra of (4-nitro-benzylidene)-(4-[1, 2, 4] triazol-1-ylmethyl-phenyl)-amine (NBTMPA) were recorded in various solvents to investigate their solvatochromic behaviour. Dipole moments of the two electronic states of NBTMPA were calculated from solvatochromic spectral shifts. These were correlated with the refractive index (n) and dielectric constant (ϵ) of various solvents. Theoretical calculations were performed to estimate the excited state dipole moment on the basis of different solvent correlation methods, like the Bilot–Kawski, Bakhshiev, Lippert–Mataga, Kawski–Chamma–Viallet and Reichardt methods. The dipole moment in the excited state was found to be higher than that in the ground state due to a substantial redistribution of electron densities and charges. Using a multiple regression analysis, the solvent–solute interactions were determined by means of Kamlet Taft parameters (α , β , π^*). Computational studies were performed by Gaussian 09 W software using a time-dependent density functional theory (TDDFT) in order to calculate the atomic charges and frontier molecular orbital energies in the solvent phase. The calculations indicated that the dipole moment of the molecule in an excited state is much higher than that in a ground state. The chemical stability of NBTMPA was determined by means of chemical hardness (η) using HOMO–LUMO energies. The reactive centres in the molecule were also identified by molecular electrostatic potential (MESP) 3D plots as a result of a TDDFT computational analysis.

© 2015 Elsevier B.V. All rights reserved.

1. Introduction

In recent years the studies on photophysical properties of several organic donor–acceptor molecules which undergo photon induced intramolecular charge transfer (PICT) have been an area of discussion in research [1–2]. When a molecule gets promoted to an excited state, a highly polar excited state is formed due to intramolecular charge transfer. Donor–acceptor (D–A) molecules can undergo rotations through D–A bonds and this makes a fluorophore very helpful in analysing the properties of the microenvironment that surrounds the molecule [3–5]. It is well known that a fluorophore containing donor–acceptor nucleus is accompanied by substantial charge redistribution upon photoexcitation. This phenomenon is a fundamental physico-chemical process that takes place in bulk solutions. Ground and excited state dipole moments of organic molecules are used to study the physico-chemical processes and to evaluate the site of nucleophilic and electrophilic

attack in photochemical reactions [6]. Various methods are available to determine the dipole moments of the solute molecules in different electronic states [7–9]. Among the existing methods, the most prominent is based on the change in position and intensity of a band in the electronic spectrum with solvents of varying polarity (Solvatochromic shift method) [10–11].

Numerous methods have been proposed for describing solvatochromism in terms of solvent characteristics and spectral parameters. The most commonly employed theoretical relations of the solvatochromic method have been given by Bilot, Lippert, Bakhshiev, Kawski, Chamma and Reichardt [12–18]. All the theories are based on the Onsager description of non-specific electrostatic solute–solvent interactions. In Onsager's reaction-field theory, the solvent is described as a dielectric continuum hosting solvent molecules within Onsager type cavities. The dipole moment of the solute polarizes the solvent so that the solute itself experiences an electric field, and the reaction field is proportional to the dipole moment of the solute in the electronic states.

In designing nonlinear optical materials, the elucidation of conformational orientations, distribution of charges and the information

* Corresponding author.

E-mail address: anitha.varghese@christuniversity.in (A. Varghese).

on dipole moments in two electronic states are of great importance. A literature survey revealed that triazole and its derivatives are extensively studied for non-linear optical properties and are developed into organic light emitting diodes due to intra molecular charge transfer [19–20]. A triazole Schiff base (azomethine) derivative bearing a coumarin nucleus was used as a fluorescent sensor for Cu^{2+} [21]. Triazolyl Schiff bases have received great attention in the pharmaceutical field due to their diverse biological behaviour [22–24]. Various triazolequinoline derivatives and their Schiff bases were reported to have antibacterial, antimicrobial and anticancer properties [25,26].

In the present work, we reported the synthesis of a novel azomethine derivative of triazole methyl aniline bearing an electron withdrawing substituent (Fig. 1). It is well established that the absorption and fluorescence spectra of the fluorophore are influenced by solvent polarity. The solvatochromic studies of the synthesized molecule were carried out by using different solvents with varying polarity. The ground and excited state dipole moments were determined using both theoretical and experimental studies. The effect of solvents on excitation and emission spectra along with solvatochromism was investigated using a multiple linear regression (MLR) analysis. In order to study the charge transfer, nucleophilic and electrophilic sites of NBTMPA with solvent, a TDDFT computational analysis were performed. The ground and excited state optimized geometries of the molecule were also performed using Gaussian software (Figs. 2 and 3).

2. Materials and methods

2.1. Theory

Most theories of solvatochromic shift in excitation and emission spectra are based on the Onsager description of non-specific electrostatic solute–solvent interactions. On the basis of quantum-mechanical second order perturbation theory, Bilot and Kawski [12,27] derived two expressions for solvatochromism as a function of refractive index and permittivity of various solvents which are given as

$$\bar{\nu}_A - \bar{\nu}_F = m^{(1)} f(n, \varepsilon) + \text{constant} \quad (1)$$

$$\bar{\nu}_A + \bar{\nu}_F = -m^{(2)} \varphi(n, \varepsilon) + \text{constant} \quad (2)$$

where $[\varphi(n, \varepsilon)] = [f(n, \varepsilon) + 2g(n)]$, the variables $m^{(1)}$ and $m^{(2)}$ are the slopes of the linear graphs from Eqs. (1) and (2).

$$m^{(1)} = \frac{2(\mu_e - \mu_g)^2}{hca^3} \quad (3)$$

$$m^{(2)} = \frac{2(\mu_e^2 - \mu_g^2)}{hca^3} \quad (4)$$

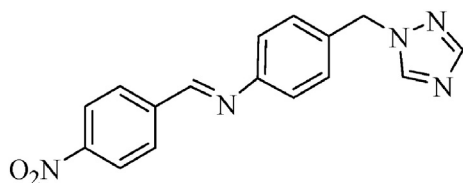


Fig. 1. Molecular structure of (4-nitro-benzylidene)-(4-[1,2,4] triazol-1-ylmethyl-phenyl)-amine.

where 'h' is the Planck's constant, 'c' is the velocity of light, 'a' is the Onsager radius and μ_g and μ_e are the dipole moments in electronic ground and excited states of the molecule. The solvent polarity functions are given by the following expressions.

$$f(n, \varepsilon) = \frac{2n^2 + 1}{n^2 + 2} \frac{\varepsilon - 1}{\varepsilon + 2} - \frac{n^2 - 1}{n^2 + 2} \quad (5)$$

$$g(n) = \frac{3}{2} \left[\frac{(n^4 - 1)}{(n^2 + 2)^2} \right] \quad (6)$$

The dipole moment in the excited state can be determined experimentally by three independent equations, proposed by Lippert–Mataga (Eq. (7)) [28,14], Bakhshiev (Eq. (8)) [29] and Kawski–Chamma–Viallet (Eq. (9)) [30,17], are given below.

$$\bar{\nu}_A - \bar{\nu}_F = m_1 F_1 + \text{constant} \quad (7)$$

$$\bar{\nu}_A - \bar{\nu}_F = m_2 F_2 + \text{constant} \quad (8)$$

$$\frac{(\bar{\nu}_A + \bar{\nu}_F)}{2} = m_3 F_3 + \text{constant} \quad (9)$$

where F_1 , F_2 and F_3 are solvent polarity functions; m_1 , m_2 and m_3 are the slopes of linear relationships which are given as follows.

$$F_1 = \frac{\varepsilon - 1}{2\varepsilon + 1} - \frac{n^2 - 1}{2n^2 + 1} \quad (10)$$

$$F_2 = \frac{2n^2 + 1}{n^2 + 2} \left[\frac{\varepsilon - 1}{\varepsilon + 2} - \frac{n^2 - 1}{n^2 + 2} \right] \quad (11)$$

$$F_3 = \left\{ \frac{2n^2 + 1}{2[n^2 + 2]} \left[\frac{\varepsilon - 1}{\varepsilon + 2} - \frac{n^2 - 1}{n^2 + 2} \right] + \frac{3[n^4 - 1]}{2[n^2 + 2]^2} \right\} \quad (12)$$

'n' and 'ε' are the refractive index and dielectric constant for selected organic solvents in the present study. The sum and difference of maximum absorbance and fluorescence wave number (cm^{-1}) is plotted against solvent polarity functions F_1 , F_2 and F_3 which gives a linear plot with gradient m_1 , m_2 and m_3 respectively, given by the following expressions.

$$m_1 = \frac{2(\mu_e - \mu_g)^2}{hca^3} \quad (13)$$

$$m_2 = \frac{2(\mu_e - \mu_g)^2}{hca^3} \quad (14)$$

$$m_3 = \frac{2(\mu_e^2 - \mu_g^2)}{hca^3} \quad (15)$$

The ground and excited state dipole moments are considered as parallel [27], provided that the molecular symmetry remains the same in both the electronic states. The following expressions were derived on the basis of Eqs. (3) and (4).

$$\mu_g = \frac{m^{(2)} - m^{(1)}}{2} \left[\frac{([hca^3])}{[2m]^{(1)}} \right]^{1/2} \quad (16)$$

$$\mu_e = \frac{m^{(2)} + m^{(1)}}{2} \left[\frac{([hca^3])}{[2m]^{(1)}} \right]^{1/2} \quad (17)$$

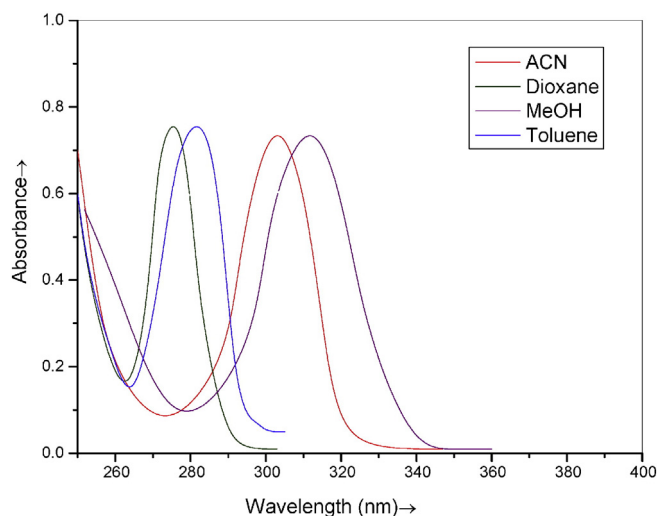


Fig. 4. Excitation spectra of NBTMPA in different organic solvents.

procured from Merck and were of spectroscopic grade. The absorption and fluorescence spectral measurements were recorded in 10^{-5} M concentration using Shimadzu UV–Visible Spectrophotometer (UV/Visible 1800) and Spectrofluorometer (RF5301PC). The analysis of solvatochromic studies was carried out using the Origin 8.0 Professional programme. Theoretical studies were performed by the TDDFT method using the Gaussian 09 W software programme.

2.2.1. Synthesis and characterization of (4-nitro-benzylidene)-(4-[1,2,4]triazol-1-ylmethyl-phenyl)-amine (NBTMPA)

An equal amount of 4-nitro benzaldehyde, **1** (1 mmol, 0.151 g), 4-(1,2,4-triazol-1-yl methyl) aniline, **2** (1 mmol, 0.174 g) and 3–4 drops of glacial acetic acid was added and refluxed in an ethanolic medium (15 mL) at 65–70 °C for 6 h (Scheme 1). The progress of the reaction was monitored using TLC with a solvent system of 3:1 ethyl acetate:n-hexane. The obtained crude solid product was filtered, washed with cold ethanol and purified by recrystallization using ethanol.

Yellow orange solid, yield–72%, m.p. 154–156 °C IR (KBr cm^{-1}): 3109 (Ar C–H str), 1372 (C–N str), 1593 (CN str) 1134 (C–N–C str), 1018 (N–N str), 1510 and 1338 (Ar–NO₂). ¹H NMR (DMSO, δ , ppm): 8.821 (s, 1 H, CHN), 8.67 (1 H, s, triazole-H) 8.376–8.354 (2 H, d, Ar–H), 8.194–8.172 (2 H, d, Ar–H), 7.997 (1 H, s, triazole–H) 7.383–7.329

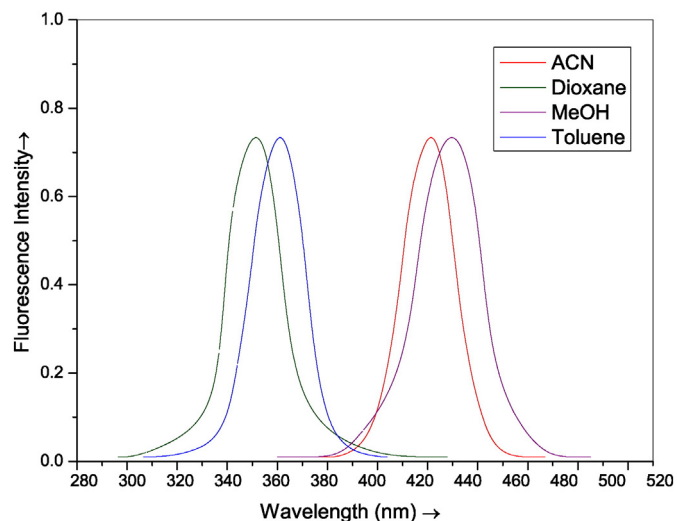


Fig. 5. Emission spectra of NBTMPA in different organic solvents.

Table 1. Analysis of solvatochromic effect for various solvents.

Solvents ^a	ν_A	ν_F	$\Delta\nu = (\nu_A - \nu_F)$	$(\nu_A + \nu_F)$	$(\nu_A + \nu_F) / 2$
Hexane	36,496	33,557	2939	70,053	35,026
1,4-Dioxane	36,101	32,894	3207	68,995	34,497
Toluene	36,231	32,467	3764	68,699	34,349
Diethylether	35,211	30,120	5091	65,331	32,665
Ethylacetate	34,364	29,069	5295	63,434	31,717
THF	33,557	27,932	5625	61,490	30,745
DCM	33,783	28,248	5535	62,032	31,016
Butanol	34,246	27,777	6469	62,024	31,012
Isopropanol	33,557	26,954	6603	60,511	30,255
Acetone	34,482	27,624	6858	62,107	31,053
Ethanol	32,573	25,252	7321	57,825	28,912
Methanol	33,444	24,875	8569	58,320	29,160
DMF	33,557	26,737	6820	60,295	30,147
Acetonitrile	33,112	25,773	7339	58,885	29,442
DMSO	31,948	25,641	6307	57,589	28,794

^a Solvents are listed in the ascending order of dielectric constants.

(m, 4 H, Ar–H), 5.455 (s, 2 H, –CH₂). ¹³C NMR (400 MHz, DMSO) δ : 51.66, 121.48, 124.00, 128.90, 129.66, 134.87, 141.40, 148.88, 150.23, 151.75, 159.22 ppm.

3. Results and discussion

3.1. Effect of solvents on excitation and emission spectra

The excitation and emission spectra were recorded in fifteen solvents ranging from non-polar to polar aprotic and to polar protic solvents at room temperature (Figs. 4 and 5). The electronic spectra of the synthesized compound were recorded in 10^{-5} M concentration. The maximum excitation and emission wavelength in cm^{-1} , the difference and sum of the spectral shifts (Stokes shift) and the average of Stokes shift values of a novel Schiff base derivative bearing an electron withdrawing group (NBTMPA) are given in Table 1. The solvent polarity functions F_1 (ϵ, n), F_2 (ϵ, n), F_3 (ϵ, n) and E_T^N for fifteen solvents are tabulated in Table 2.

From Table 1 it is clear that for NBTMPA, when the solvent polarity increases from non-polar to polar solvent (n-hexane to methanol) the maximum absorption wavelength shifts from 3 nm to 25 nm. This is due to π – π^* transitions along with the charge transfer of the conjugated core. The emission spectrum of NBTMPA shows a larger red spectral shift indicating that the energy of the ground state is less influenced by increasing the solvent polarity compared to the energy of the excited

Table 2. Values of solvent polarity functions using different correlation methods.

Solvent	F_1 (ϵ, n) ¹	F_2 (ϵ, n) ²	F_3 (ϵ, n) ³	E_T^N ⁴
n-Hexane	–0.00136	–0.00252	0.25378	0.009
1,4-Dioxane	0.02451	0.04990	0.31162	0.164
Toluene	0.01323	0.02907	0.34990	0.099
Diethylether	0.16674	0.37658	0.42823	0.117
Ethylacetate	0.19963	0.48908	0.49791	0.228
THF	0.20957	0.54907	0.55113	0.207
DCM	0.21713	0.59033	0.58296	0.321
Butanol	0.26347	0.75042	0.64655	0.602
Isopropanol	0.27217	0.76160	0.63739	0.546
Acetone	0.28430	0.79037	0.63936	0.355
Ethanol	0.28874	0.81293	0.65245	0.654
Methanol	0.30855	0.85460	0.65104	0.762
DMF	0.27438	0.83556	0.70980	0.386
Acetonitrile	0.30659	0.86391	0.66421	0.460
DMSO	0.26308	0.84038	0.74416	0.444

¹ Lippert–Mataga bulk solvent polarity function.

² Bakshiev bulk solvent polarity function.

³ Kawski–Chamma–Viallet bulk solvent polarity function.

⁴ Reichardt microscopic solvent polarity function.

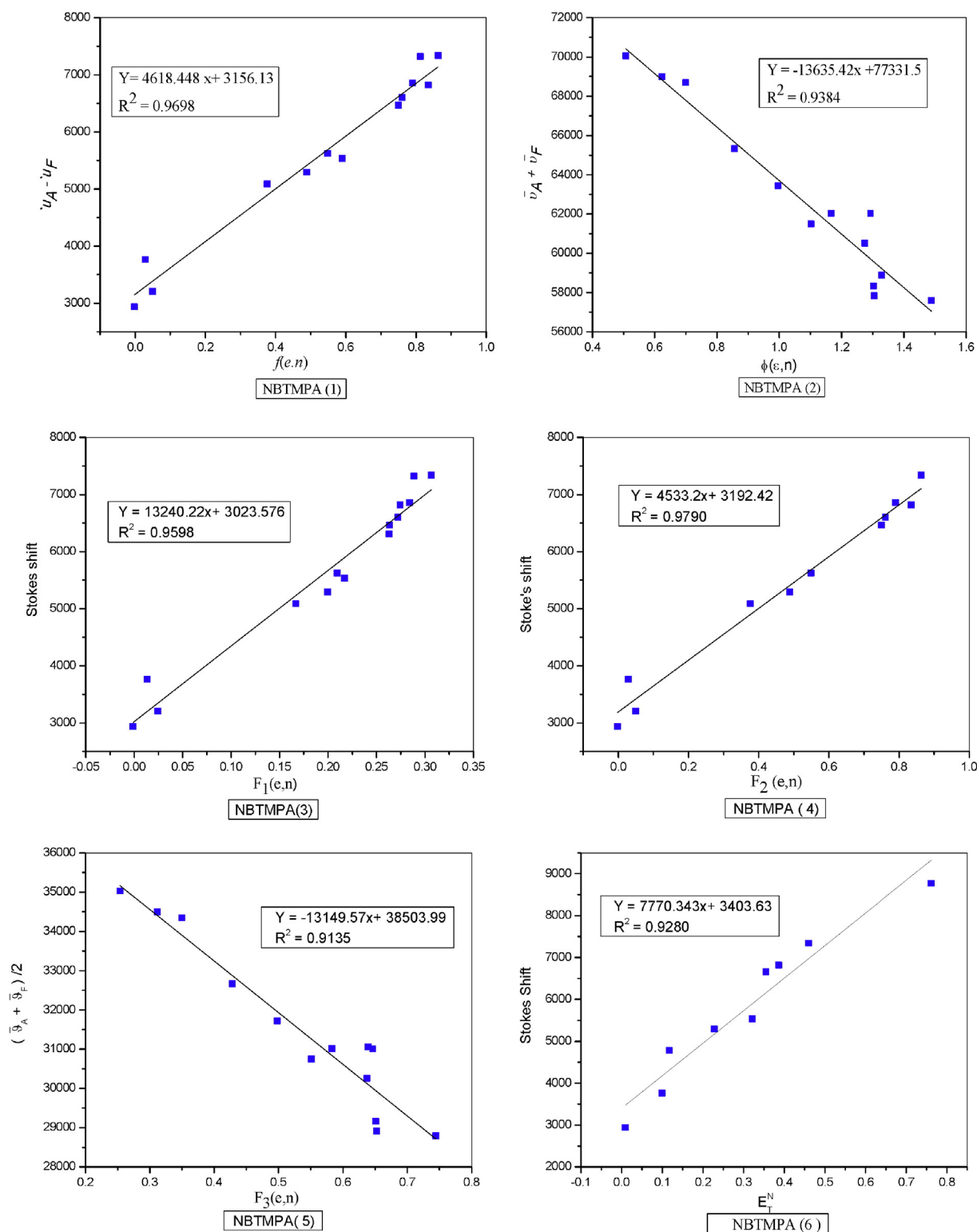


Fig. 6. Linear plots of Bilot–Kawski (1) and (2), Lippert–Mataga (3), Bakhshiev (4), Kawski–Chamma–Viallet (5) and Reichardt (6) correlation methods of solvent polarity functions $f(\epsilon, n)$, $\phi(\epsilon, n)$, $F_1(\epsilon, n)$, $F_2(\epsilon, n)$, $F_3(\epsilon, n)$ and E_T^N against $(\bar{\nu}_A - \bar{\nu}_F)$, $(\bar{\nu}_A + \bar{\nu}_F)$, $(\bar{\nu}_A + \bar{\nu}_F) / 2$.

state. Increasing the solvent polarity enhances the stoke shift values from 2939 cm^{-1} to 8569 cm^{-1} for n-hexane to methanol respectively. For a polar aprotic solvent, dimethyl sulfoxide and a polar protic solvent, methanol the stoke shift values were found to be 6307 cm^{-1} to 8569 cm^{-1} respectively. These data implies that the molecule is influenced by solvent parameters such as polarity, hydrogen bond donor

and hydrogen bond acceptor strength. It also reveals that in polar solvents the molecule is more stabilized in the excited state than in the ground state and the expected value for the excited state dipole moment would be higher. The weaker spectral red shifts of the excitation spectrum with increasing solvent polarity are due to the fact that the Schiff base derivative are more polarized in the excited state than the

Table 3.
Statistical data of linear plots for different correlation methods of NBTMPA.

Compound	Method	Slope (m)	Intercept (c)	Correlation Coefficient (R ²)	N ^b
NBTMPA	Bilot–Kawski (1)	$m^{(1)} = 4618.44$	3156.13	0.9698	13
	Bilot–Kawski (2)	$m^{(2)} = 13,635.42$	77331.5	0.9384	13
	Lippert–Mataga	$m_1 = 13,240.22$	3023.57	0.9598	14
	Bakhshiev	$m_2 = 4533.2$	3192.42	0.9790	11
	Kawski–Chamma–Viallet	$m_3 = 13,149.57$	38503.99	0.9135	13
Reichardt	$m_4 = 7770.343$	3403.63	0.9280	9	

^b Number of data.

ground state. Thus the excitation spectra are less sensitive to the effect of solvent polarity as compared to the emission spectra.

3.2. Experimental and theoretical calculations of dipole moments

To study the solvatochromism of NBTMPA, the spectral parameters are found to be correlated with different solvent polarity methods. By employing Bilot–Kawski, Lippert–Mataga, Bakhshiev, Kawski–Chamma–Viallet and Reichardt linear correlations, linear graphs of $(\bar{\nu}_A - \bar{\nu}_F)$ and $(\bar{\nu}_A + \bar{\nu}_F)$ were plotted against $f(\epsilon, n)$ and $\rho(\epsilon, n)$ respectively, the Stokes shift and its mean $\{(\bar{\nu}_A - \bar{\nu}_F)$ and $(\bar{\nu}_A + \bar{\nu}_F) / 2\}$ Table (1) of NBTMPA (Fig. 6) are plotted against polarity functions $F_1(\epsilon, n)$, $F_2(\epsilon, n)$, $F_3(\epsilon, n)$ and E_T^N (Table 2).

The slopes, intercepts, correlation coefficients and the data of different solvent correlation methods from Fig. 6 are summarized in Table 3. The higher correlation coefficient values (greater than 0.90) suggest better linearity for these methods. The ground state and excited state dipole moments are calculated from the slopes of the linear graphs of Bilot–Kawski method using Eqs. (16) and (17). By applying Eqs. (13) to (15) and (22) of Lippert–Mataga, Bakhshiev, Kawski–Chamma–Viallet and Reichardt solvatochromic shift methods, the excited dipole moment can be estimated from the respective slopes. The quantum yield of NBTMPA was calculated using single point method by comparing the integrated intensity and optical density of the sample to that of a reference compound, anthracene in ethanol at room temperature. The quantum yield (Φ) of NBTMPA was determined by the following relation and is expressed as.

$$\Phi = \Phi_{std} \times \frac{I_S}{I_R} \times \frac{OD_R}{OD_S} \times \frac{\eta_S^2}{\eta_R^2}$$

Where Φ_{std} is the quantum yield of reference standard (0.27 from literature), I_S and I_R are the integrated fluorescence intensity of sample and reference standard, OD_S and OD_R are the optical densities of sample and standard, and η_S^2 and η_R^2 are the square of refractive indices of solvent respectively. The ratio of square of the refractive indices was found to be 1. The calculated quantum yield (Φ) of NBTMPA was found to be 0.205 [36]. The spectral properties like fluorescence maxima, quantum yield are controlled by inter molecular hydrogen bonding. The Onsager cavity radius of NBTMPA was calculated by means of Vander Waal's

volume using Edward's atomic increment method. The Onsager cavity radius (a) of NBTMPA is calculated by the following expression [37].

$$a = \left[\frac{3M}{4\pi\delta N_A} \right]^{1/3} \quad (25)$$

where M is the molecular weight of solute, δ is the density of the solute and N_A is the Avogadro's number.

From Table 4, it is observed that the excited state dipole moments (μ_e) of NBTMPA are higher than the ground state dipole moments (μ_g). The calculated values for excited state dipole moments using Bilot–Kawski, Bakhshiev and Reichardt correlation methods are comparatively in good agreement. The excited state dipole moment calculated by Lippert–Mataga and Kawski–Chamma–Viallet method is slightly higher than the values obtained by the earlier correlation methods, as these does not consider the effect of solute polarizability. The difference in dipole moment can be explained on the basis of charge transfer (CT) and nature of the emitting state. By using Eqs. (16) and (17) the ground and excited state dipole moments of NBTMPA were calculated by assuming that the dipole moments are almost parallel [38]. So we have estimated the angle between the dipole moments using Eq. (19) which was found to be 0° implying that they are parallel. The ground state dipole moment was calculated using theoretical ab initio calculations by Gaussian 09 W software and Bilot–Kawski correlation method. From Table 4, μ_g calculated from both methods are fairly in good agreement. Using TD–DFT analysis the ground and excited dipole moments were estimated as $\mu_g = 3.7$ D and $\mu_e = 6.9$ D indicating that the molecule is in a polar excited state. Also, the solvent used was found to be in a more stabilized state. The calculated values for the dipole moments in the two electronic states are $\mu_g = 5.7$ D and $\mu_e = 11.5$ D suggesting a more polar excited state for the molecule. This also implies that the interactions between solute and solvent are stronger in the excited state which leads to a change in the distribution of charge densities. Using Eq. (18) the ratio of dipole moment in the excited state to the dipole moment in the ground state was found to be 2.02.

PICT has been used to explain the charge separation in NBTMPA. 1, 2, 4-Triazole nucleus does not produce any significant change in the movement of π electrons. The intramolecular charge transfer state is

Table 4.
Dipole moments in two electronic states (Debye) of NBTMPA.

Compound	Onsager radius ^a	μ_g^b	μ_g^c	μ_e^d	μ_e^e	μ_e^f	μ_e^g	μ_e^h	μ_e^i
NBTMPA	4.06	3.7	5.7	6.9	11.5	13.6	9.48	13.55	7.64

^a Onsager radius of NBTMPA using Edward's atomic increment method.

^b Dipole moment in the ground state calculated by Gaussian software.

^c Dipole moment in the ground state calculated using Bilot–Kawski method (Eq. (16)).

^d Dipole moment in the excited state calculated by Gaussian software.

^e Dipole moment in the excited state calculated using Bilot–Kawski method (Eq. (17)).

^f Dipole moment calculated using Lippert Mataga method (Eq. (13)).

^g Dipole moment calculated using Bakhshiev method (Eq. (14)).

^h Dipole moment calculated using Kawski–Chamma–Viallet method (Eq. (15)).

ⁱ Dipole moment calculated using Reichardt method (Eq. (22)).

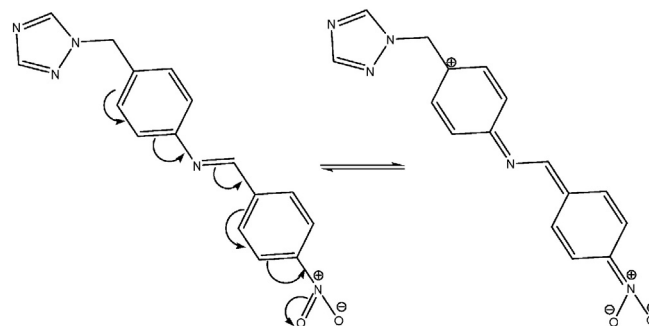


Fig. 7. Canonical structures of NBTMPA.

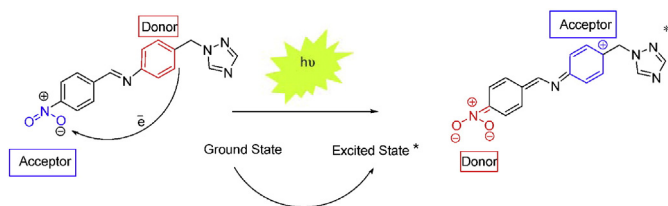


Fig. 8. Photon induced intramolecular charge transfer (PICT) of NBTMPA as donor–acceptor (D–A) molecule.

formed when a substantial amount of charge is transferred from benzyl ring to nitro group through an azomethine linkage upon excitation. This makes the nitro group a strong electron donor and benzylic ring a strong electron acceptor (Fig. 7). This also indicates that the molecule becomes more polarized in the excited state than in the ground state.

NBTMPA is an example for donor–acceptor molecule, which consists of both electron donating and acceptor groups within a molecule. When NBTMPA absorbs a photon and gets promoted into the excited state the electron from the benzylic ring (donor) migrates towards the nitro group (acceptor). This results in a highly polar state or CT state making the benzyl ring a strong electron acceptor and the nitro group a strong electron donor in the excited state. The dipole moment of NBTMPA at the excited state is twice as much as it is when in the ground state. This difference in the dipole moments across the two electronic states can be explained on the basis of intramolecular charge transfer (ICT). It indicates that the charge transfer in excited state is accompanied by photon induced intramolecular charge transfer (PICT). Thus due to PICT (Fig. 8) the planarity of the molecule decreases on excitation, which also renders the molecule more polar in the excited state as compared to the ground state [39].

3.3. Computational analysis

The direction of charge transfer can be estimated on the basis of frontier molecular orbitals. HOMO and LUMO energies were calculated in an ethanolic medium which provides the information regarding the charge transfer within the molecule. The electron donating ability is characterized by HOMO, whereas electron acceptor ability is characterized by LUMO. The difference in the HOMO and LUMO energies gives information about the chemical stability of the molecule. If the HOMO–LUMO energy gap is small, the HOMO electrons can be easily excited to the LUMO orbitals. The highest occupied and lowest unoccupied molecular orbitals energies were computed in ethanol as -0.239 and -0.106 a.u. respectively. The HOMO and LUMO 3D plots of NBTMPA are shown in Fig. 9. From HOMO–LUMO plots, the red region corresponds to the positive phase and the blue region corresponds to the negative phase. It was observed that HOMO is localized on azomethine linkage and benzylic ring, whereas LUMO is localized over the entire molecule except for methylene group and 1, 2, 4-triazole nucleus.

The chemical stability of a molecule gives significant information about the chemical hardness (η) of a molecule. The hardness of the molecule can be estimated by using highest occupied molecular orbital (HOMO) and lowest unoccupied molecular orbital (LUMO) energies.

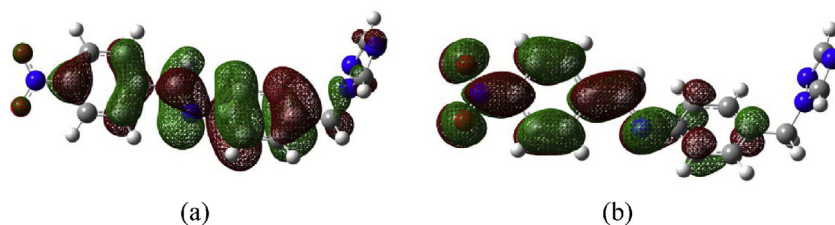


Fig. 9. HOMO (a) and LUMO (b) 3D plots computed by TDDFT studies for NBTMPA. (For interpretation of the references to colour in this figure, the reader is referred to the web version of this article.)

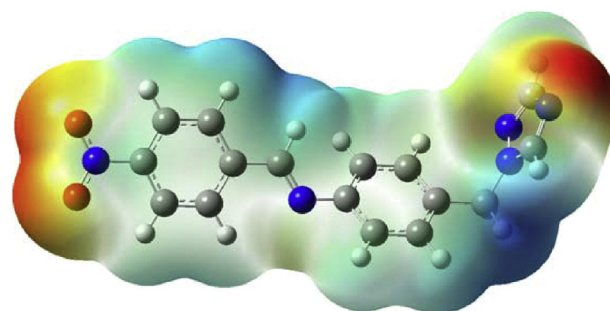


Fig. 10. Molecular electrostatic potential (MESP) plot of NBTMPA. (For interpretation of the references to colour in this figure, the reader is referred to the web version of this article.)

The molecules possessing a large energy gap between HOMO–LUMO energies are known as hard, whereas molecules possessing a small energy gap are known as soft molecules. Soft molecules require very little energy for excitation and thus they are more polarized than hard molecules. The chemical hardness (η) can be estimated by the following expression [40].

$$\eta = \frac{[E_L - E_H]}{2} \quad (26)$$

Where E_H and E_L are the HOMO and LUMO energies of respective frontier molecular orbitals. The hardness of the molecule was found to be -0.133 a.u. Thus we can conclude that from the estimated value the molecule has comparatively small energy gap which indicates that the molecule, NBTMPA is soft.

The molecular electrostatic potential (MESP) plot given in Fig. 10 provides the information for determining a suitable position for nucleophilic and electrophilic attack along with the hydrogen bonding interactions of solvent. Different colours in the MESP plot symbolize the different values of electrostatic potential at the surface. The negative phase in the MESP plot is represented in red colour which can be related to the electrophilic site, and the positive phase is represented in blue colour corresponds to the nucleophilic site. From the MESP plot, the negative phases are localized in nitro group and 1, 2, 4-triazole nucleus and positive phases are enclosed by benzylic ring, azomethine linkage and all hydrogen atoms.

Theoretical calculations by Gaussian 09 W software were used to determine the ground state dipole moment of NBTMPA. The information regarding the charge distribution was obtained from the atomic charges of each atoms of NBTMPA and the analysis was performed in ethanol. In solvent medium, O atoms (35,36), nitrogen atoms except (N-34) and most of the carbon atoms carry a significant negative charge, which act as donor atoms; while C (1), C (2), C (11), C (18), C (22), C (24), C (30) and N (34) atoms carry a positive charge, which act as acceptor atoms. In solvent medium the distribution of charge directs from N (34) to C (14) atoms having magnitude $+0.388$ eV to -0.133 eV respectively. Due to this charge separation of the molecule, NBTMPA will be more polarized in the excited state. This charge transfer phenomena

Table 5.
Kamlet–Taft parameters values for multiple linear regression analysis.

Solvents	A	B	π^*
Hexane	0	0	−0.081
1,4-Dioxane	0	0.37	0.55
Toluene	0	0.11	0.54
Diethyl ether	0	0.47	0.27
Ethyl acetate	0	0.45	0.55
THF	0	0.55	0.58
DMSO	0	0.76	1
DMF	0	0.69	0.88
DCM	0.3	0	0.82
Butanol	0.79	0.88	0.47
Isopropanol	0.76	0.84	0.48
Acetone	0.08	0.48	0.71
Ethanol	0.83	0.77	0.54
Methanol	0.93	0.62	0.6
Acetonitrile	0.19	0.31	0.75

gives rise to a difference in ground state and excited state dipole moments. The atomic charges of all hydrogen atoms exhibit a positive charge in ethanol, indicating that it can donate electrons from hydrogen atom to other atoms. These investigations confirm the results from multiple linear regression analysis.

3.4. Multiple linear regression analysis

Multiple linear regression analysis provides the information on different types of interactions between solute and solvent. It is also used to explain the mechanism of electronic transition. From the existing literature, it is well known that the intensity, position and shape of the absorption spectrum can explain the spectral shifts with the nature of solvent and solute. The spectral shifts induced by solvents were calculated using Kamlet–Taft parameters such as α , β and π^* . In order to get more information on the solvatochromic properties of NBTMPA, the spectral properties were correlated with Kamlet–Taft parameters. The wave numbers of absorption ($\bar{\nu}_A$), fluorescence ($\bar{\nu}_F$) and Stokes shift ($\bar{\nu}_A - \bar{\nu}_F$) were correlated with α , β and π^* using multiple linear regression analysis. This analysis is used to explain the mechanism of transitions between ground and excited states based on the information of solvent–solute interactions. The values of Kamlet–Taft parameters (α , β and π^*) are tabulated in Table 5.

The regression analysis with correlation coefficient is given in Eq. (27).

$$\left. \begin{aligned} \bar{\nu}_A &= 39972 - 2231\alpha - 5245\beta + 6111\pi^*; r = 0.79 \\ \bar{\nu}_F &= 40164 - 7046\alpha - 7357\beta - 13736\pi^*; r = 0.82 \\ \Delta\bar{\nu} &= 2307 + 5244\alpha + 2833\beta + 8514\pi^*; r = 0.75 \end{aligned} \right\} \quad (27)$$

From the above equations, it was observed that the coefficient of π^* is significantly higher than the coefficients of α and β . Therefore the non-specific dielectric interaction, π^* of solvents has a major influence on solute–solvent interactions. In this case, π^* is more powerful than HBD (α) and HBA (β). This implies that the excitation and emission spectral shifts are controlled by polarity/dipolarizability of non-specific interactions. However the relatively higher values of HBA hydrogen bond acceptor strength (β), cannot be neglected. The HBA (β) influence is more than HBD (α). From MLR analysis, it is clear that $\bar{\nu}_A$ and $\bar{\nu}_F$ have relatively good correlation coefficients. The relatively higher values of π^* and β reveal that the excitation and emission spectrum shows a bathochromic shift or positive solvatochromism (red shift). Also, the higher values of π^* and β in the fluorescence wavelength in cm^{-1} , $\bar{\nu}_F$ clearly explains the fact that it undergoes a large bathochromic or red shift as compared to the excitation spectrum. This also gives evidence that the molecule NBTMPA is more polarized in the excited state than in the ground state. Therefore, the dipole moment of NBTMPA in the excited state would be higher than the dipole moment in the ground

state. These interpretations of multiple linear regression analysis can be confirmed on the basis of results tabulated in Table 4.

4. Conclusion

A novel azomethine derivative containing 1, 2, 4-triazole moiety bearing an electron withdrawing substituent was synthesized and characterized by ^1H NMR, IR and UV spectral studies. The effect of solvents in excitation and emission spectra was analysed using different solvent polarity correlation methods. We have estimated the dipole moment in the ground state by using both Gaussian 09 W Software and Bilot–Kawski method. The dipole moment in the excited state was determined by Bilot–Kawski, Lippert–Mataga, Bakhshiev, Kawski–Chamma–Viallet, and Reichardt correlation methods. In all the methods the dipole moment in the excited state for NBTMPA were found to be higher than the ground state dipole moment. This implies that NBTMPA is more polar or stable in the excited state than in the ground state. This also indicates that the azomethine derivative has a more relaxed excited state due to photon induced intramolecular charge transfer (PICT). Computational studies were performed using TDDFT calculations which imply that the molecule, NBTMPA has both nucleophilic and electrophilic sites. Thus NBTMPA can serve as a promising candidate for luminescence materials, fluorescent probes and non-linear optical materials. Multiple linear regression analysis was performed to investigate the interaction between solvent and solute. Both the excitation and emission spectra were controlled by polarity/dipolarizability of non-specific interactions (π^*) of solvent.

Acknowledgements

The authors are grateful to D Sravan Kumar Perumalla (IISC, Bangalore, India) for computational analysis. Author would also like to thank NMR Research Centre (IISC, Bangalore, India) for the spectral analysis.

References

- [1] Z.R. Grabowski, K. Rotkiewicz, W. Rettig, Chem. Rev. 103 (2003) 3899–4032.
- [2] S. Arzhantsev, K.A. Zachariasse, M. Maroncelli, J. Phys. Chem. 110 (2006) 3454–3470.
- [3] S. Tazuke, R. Hayashi, C. Frank, Chem. Phys. Lett. 135 (1987) 123–127.
- [4] J. Paczkowski, D.C. Neckers, Macromolecules 24 (1991) 3013–3016.
- [5] A. Bajorek, J. Paczkowski, Macromolecules 31 (1998) 86–95.
- [6] A. Rahabi, M.M. Chebli, S.M. Hamdi, A.M.S. Silva, D. Kheffache, B.B. Kheddis, M. Hamdi, J. Mol. Liq. 195 (2014) 240–247.
- [7] J. Czekella, Z. Elektrochem. 64 (1960) 1221–1228.
- [8] A. Kawski, B. Kukliński, P. Bojarski, Z. Naturforsch 57a (2002) 716–722.
- [9] J. Czekella, Chimia 15 (1961) 26–31.
- [10] S.K. Patil, M.N. Wari, C.Y. Panicker, S.R. Inamdar, Int. J. Adv. Res. 1 (2013) 616–626.
- [11] M.A. Rauf, S. Hisaindee, J. Mol. Struct. 1042 (2013) 45–56.
- [12] L. Bilot, A. Kawski, Z. Naturforsch. 17a (1962) 621–627.
- [13] E. Lippert, Ber. Bunsenges. Phys. Chem. 61 (1957) 962–975.
- [14] N. Mataga, Y. Kaifu, M. Koizumi, Bull. Chem. Soc. Jpn. 29 (1956) 465–470.
- [15] N.G. Bakhshiev, Opt. Spektrosk. 10 (1961) 717–726.
- [16] A. Kawski, B. Kukliński, P. Bojarski, Chem. Phys. Lett. 415 (2005) 251–255.
- [17] A. Chamma, P. Viallet, C.R. Hebr, Seances Acad. Sci. Ser. France 270 (1970) 1901–1904.
- [18] C. Reichardt, Chem. Rev. 94 (1994) 2319–2358.
- [19] J. Lee, K. Shizu, H. Tanaka, H. Nomura, T. Yasuda, C. Adachi, J. Mater. Chem. C 1 (2013) 4599–4604.
- [20] Y.-B. Ruan, Y. Yu, C. Li, N. Bogliotti, J. Tang, J. Xie, Tetrahedron 69 (2013) 4603–4608.
- [21] W. Wang, W.-J. Yuan, Q.-L. Liu, Y.-N. Lei, S. Qi, Y. Gao, Heterocycl. Commun. 20 (5) (2015) 289–292.
- [22] H. Bayrak, A. Demirbas, S.A. Karaoglu, N. Demirbas, Eur. J. Med. Chem. 44 (2009) 1057–1066.
- [23] B.S. Creaven, M. Devereux, A. Foltyn, S. McClean, G. Rosair, V.R. Thangella, M. Walsh, Polyhedron 29 (2010) 813–822.
- [24] R.H. Chandramouli, V. Udipi, H. Bindu, Orient. J. Chem. 23 (3) (2007) 1077–1080.
- [25] H. Bektas, N. Karaali, D. Sahin, A. Demirbas, S.A. Karaoglu, N. Demirbas, Molecules 15 (2010) 2427–2438.
- [26] M. Clemons, E.R. Coleman, S. Verma, Cancer Treat. Rev. 30 (2004) 325–332.
- [27] A. Kawski, in: J.F. Rabek (Ed.), Progress in Photochemistry and Photophysics, 5, CRC Press, Boca Raton, USA 1992, pp. 1–47.
- [28] E. Lippert, Z. Naturforsch A Phys. Sci. 10 (1955) 541–545.
- [29] N.G. Bakhshiev, Opt. Spektrosk. 16 (1964) 821–832.
- [30] A. Kawski, Acta Phys. Polon. 29 (1966) 507–518.

- [31] A. Kowski, Z. Naturforsch. 57 (a) (2002) 255–262.
- [32] J.L. Abboud, M.J. Kamlet, R.W. Taft, J. Am. Chem. Soc. 99 (1977) 8325–8327.
- [33] F.W. Oowler, A.R. Katritzky, R.J.D. Rutherford, J. Chem. Soc. B (1971) 460–469.
- [34] M.J. Kamlet, M.E. Jones, R.W. Taft, J. Chem. Soc. Perkin Trans. 2 (3) (1979) 349–356.
- [35] M.J. Kamlet, R.W. Taft, J. Am. Chem. Soc. 98 (1976) 377–383.
- [36] J.R. Lakowicz, Principles of Fluorescence Spectroscopy, third ed. Springer, New York, 2006.
- [37] P. Suppan, Chem. Phys. Lett. 3 (1983) 272–275.
- [38] Y.G. Sidir, I. Sidir, Spectrochim. Acta A Mol. Biomol. Spectrosc. 102 (2013) 286–296.
- [39] C. Zhong, Phys. Chem. Chem. Phys. 17 (2015) 9248–9257.
- [40] R.M. Silverstein, G.C. Bassler, T.C. Morill, Spectrometric Identification of Organic Compounds, fourth ed. Wiley, New York, 1981 249–304.